Plant Cell Reports (2026) 45:90
https://doi.org/10.1007/s00299-026-03775-z

ORIGINAL ARTICLE

6 mA methylation differences in *Riccia fluitans* organellar genomes under flood stress

Mateusz Maździarz[1] · Katarzyna Krawczyk[1] · Paweł Sulima[2] · Jakub Sawicki[2]

Received: 6 November 2025 / Accepted: 6 March 2026 / Published online: 14 March 2026

Key message **The first genome-wide evidence of 6 mA methylation in the organellar genomes of *Riccia fluitans* was provided by this study, with methylation patterns being shown to differ between aquatic and terrestrial forms, suggesting that epigenetic regulation is involved in environmental adaptation.**

Abstract DNA N⁶-methyladenine (6 mA) has recently emerged as an important epigenetic mark associated with transcriptional regulation and stress adaptation in plants. However, its role in organellar genomes remains poorly understood, especially in early-diverging lineages. The amphibious liverwort *Riccia fluitans* offers a unique opportunity to investigate environmentally induced epigenetic plasticity, as it can reversibly transition between terrestrial and aquatic morphotypes. Using Oxford Nanopore native DNA sequencing, we profiled 6 mA methylation across plastid and mitochondrial genomes of *Riccia fluitans* cultivated under aquatic and terrestrial conditions, and integrated these data with Illumina RNA-seq-based gene expression profiles. We identified 6 mA methylation sites characteristic of each habitat, with a markedly higher frequency of methylation in the aquatic form. Several differentially expressed genes (e.g., *accD*, *psbA*) were co-located with environment-specific methylation sites, suggesting potential spatial association between differential methylation and gene expression. Our results provide the first evidence of environmentally responsive organellar 6 mA methylation in a bryophyte, highlighting a previously unrecognized layer of epigenetic control that may contribute to the adaptive plasticity of early land plants.

Graphical Abstract

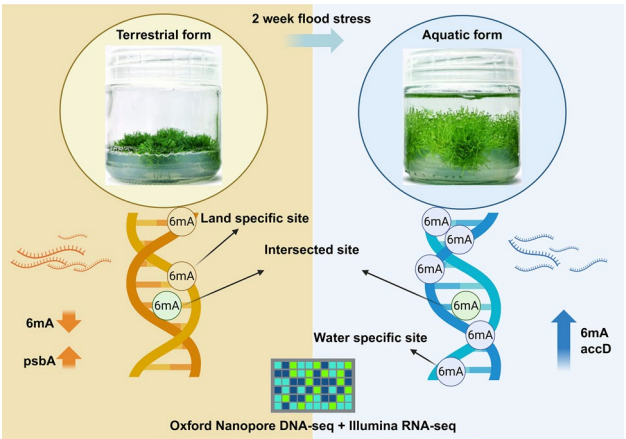

Keywords *Riccia fluitans* · N⁶-methyladenine · Gene expression

Communicated by Csaba Máthé.

Extended author information available on the last page of the article

Introduction

The transition of plants from aquatic to terrestrial habitats over 450 million years ago required fundamental molecular and physiological innovations that enabled desiccation tolerance, efficient gas exchange, and structural support on land (Clark et al. 2022). Among extant bryophytes, several lineages still exhibit ancestral forms of developmental plasticity that reflect early mechanisms of environmental responsiveness (Paukszto et al. 2023). The liverwort *Riccia fluitans* (*R. fluitans*) L. is an exceptional example of such plasticity. It displays two distinct morphotypes that can reversibly develop under contrasting conditions: a thin, simple, submerged thallus in water and a thicker, air-exposed thallus with epidermal differentiation, pores, and cuticle under terrestrial conditions (Althoff & Zachgo 2020; Althoff et al. 2022). This capacity for environmentally induced morphological and transcriptional reprogramming makes *R. fluitans* a powerful model for studying molecular adaptation to fluctuating habitats in early land plant lineages.

Epigenetic mechanisms have emerged as critical regulators of plant stress responses and adaptive plasticity. They mediate reversible but sometimes heritable modifications in gene expression through DNA methylation, histone modification, and RNA-associated pathways (Liu et al. 2014; Arora et al. 2022). DNA methylation, in particular, is essential for genome stability and environmental "stress memory." While the majority of studies in plants have focused on 5-methylcytosine (5mC), increasing evidence demonstrates that N^6-methyladenine (6 mA) also contributes to epigenetic regulation (Liu & He 2020). In angiosperms such as *Arabidopsis thaliana* and *Oryza sativa*, 6 mA has been shown to occur within gene bodies and to correlate positively with gene expression, suggesting a potential role in transcriptional activation (Arora et al. 2022). The abundance of 6 mA can also change in response to abiotic stress and environmental shifts, implicating it in plant adaptation.

In contrast to nuclear genomes, the presence and functional role of 6 mA in organellar DNA remain poorly understood. Chloroplasts and mitochondria are central to photosynthesis, respiration, and redox regulation, and both genomes exhibit transcriptional plasticity during stress adaptation. Recent analyses based on long-read sequencing and sensitive detection algorithms revealed low but detectable levels of 6 mA in plant organelles, including *A. thaliana* and *O. sativa*, suggesting that adenine methylation might contribute to the fine-tuning of organellar gene expression and genome maintenance (Li et al. 2020a; Yuan et al. 2020). However, comprehensive maps of organellar 6 mA under changing environmental conditions have not yet been produced for any early-diverging plant lineage.

Table 1 Summary of sequencing data: mapped reads and coverage depth for the plastid and mitochondrial genomes of *R. fluitans*

Sample	Plastome (mapped/coverage)	Mitochondrial (mapped/coverage)
L1	121,188 / 622.879	42,044 / 122.996
L2	6,100,464 / 7382.22	672,374 / 1385.19
L3	11,820,298 / 7438.09	1,189,466 / 1354.74
L4	1,964,711 / 5957.23	273,945 / 780.677
W1	2,995,380 / 7387.19	272,438 / 1019.81
W2	3,564,524 / 7894.53	376,578 / 2305.14
W3	16,502,769 / 7914.79	2,719,788 / 4777.82
W4	9,290,389 / 7911.63	1,484,200 / 3053.77

The recent advances in Oxford Nanopore Technologies (ONT) have enabled direct detection of DNA base modifications from native DNA reads, providing single-molecule resolution and eliminating the need for chemical or antibody-based conversion (Rang et al. 2018; Wang et al. 2021). ONT sequencing measures characteristic changes in ionic current as DNA passes through a biological nanopore, and these electrical signals are influenced by both the identity and chemical state of nucleotides within a short 5–6 bp context window. Modified bases such as N^6-methyladenine (6 mA) can alter this signal profile, allowing their identification through machine-learning models trained on methylated and unmethylated control datasets (Wang et al. 2021).

The accuracy of ONT-based modification detection has markedly improved with the introduction of neural network basecallers, which integrate modified-base recognition directly into sequence prediction. Comparative analyses have demonstrated that ONT-derived 6 mA frequencies show a strong correlation with independent orthogonal methods, including PacBio single-molecule real-time (SMRT) sequencing and mass spectrometry–based quantification (Karst et al. 2021; Wang et al. 2021). Importantly, ONT preserves strand information and enables quantification of methylation stoichiometry at single-nucleotide resolution across biological replicates (Rang et al. 2018).

The amphibious *R. fluitans* provides an ideal system to explore how 6 mA methylation participates in organellar-level epigenetic regulation under environmental transitions. Previous studies demonstrated significant differences between aquatic and terrestrial morphotypes at the transcriptomic and epitranscriptomic levels, including enhanced accumulation of N6-methyladenosine (m^6A), m5C, and pseudouridine (Ψ) modifications in the aquatic form, as well as elongation of poly(A) tails in nuclear transcripts (Maździarz et al. 2024; Maździarz et al. 2025a, b). These observations indicate that environmentally induced changes in *R. fluitans* involve coordinated epigenetic and post-transcriptional responses.

Here, we hypothesized that 6 mA methylation constitutes a regulatory layer within organellar genomes that modulates gene expression in response to environmental change. Specifically, we predicted that the aquatic form of *R. fluitans*, subjected to altered oxygen availability, light quality, and metabolic flux, would exhibit distinct 6 mA methylation patterns in its plastid and mitochondrial genomes compared to the terrestrial form. To test this, we applied Oxford Nanopore native DNA sequencing to generate high-resolution 6 mA methylation profiles for both organellar genomes and integrated them with RNA-seq-based gene expression data. This work represents the first comprehensive characterization of organellar 6 mA dynamics in a bryophyte, providing new insights into the epigenetic mechanisms underlying the environmental plasticity of early land plants.

Materials and methods

Plant material and sequencing

Plants were grown in vitro, following the method described in our previous works (Sawicki et al. 2023; Maździarz et al. 2024). Four-week-old in vitro cultures of *R. fluitans* were divided into two experimental groups. In the first group, four cultures were maintained under terrestrial conditions (L1–L4), whereas in the second group, four cultures were cultivated under submerged conditions (W1–W4). For both groups, light intensity was supplied at 35 µmol m^{-2} s^{-1} photons emitted by cool-white fluorescent lamps. After two weeks of cultivation, material was collected from the samples, and DNA isolation was performed. DNA was isolated from plant material using the DNeasy Plant Kit (Qiagen) and further purified with the Genomic DNA Purification Kit (New England Biolabs), according to the manufacturers' protocols. Sample purity was assessed spectrophotometrically with a Cary 60 spectrophotometer (Agilent), while DNA concentration was determined with a Qubit fluorometer and Qubit™ dsDNA BR Assay Kit (Invitrogen). Fragment length distribution and integrity were evaluated using the TapeStation system with Genomic DNA ScreenTape Assay (Agilent). Long-read libraries were prepared using the Ligation Sequencing gDNA – Native Barcoding Kit 24 V14 (Oxford Nanopore Technologies, ONT) and sequenced on a PromethION P2 Solo device (ONT) with R10.4.1 flow cells (FLO-PRO114M). Two barcoded libraries were loaded onto a single flow cell for sequencing.

Methylation 6 mA analysis

DNA-seq long reads were subjected to the sup basecalling process using dorado v.0.9.5 (https://github.com/nanoporetech/dorado) with the 6 mA methylation option. The resulting BAM files were mapped to the plastid (OR220797.1) and mitochondrial (OR220799.1) genomes of *R. fluitans* using the dorado aligner function. Subsequently, the BAM files were sorted and indexed using the Samtools v.1.12 tool (Li et al. 2009). Ultimately, information about per-base methylation was obtained using the Modkit v.0.2.7 tool (https://github.com/nanoporetech/modkit). Methylation sites were separated by strand to avoid situations where two different sets of methylated reads were present at the same site. Methylation sites were filtered to ensure that at least three out of four replicates in either the aquatic or terrestrial *R. fluitans* had more than ten methylated reads and a fraction modified greater than 20. Next, sites that did not pass the filters in the aquatic form were classified as specific to the terrestrial form, while sites without their counterparts in the terrestrial condition were assigned to the aquatic form. The intersected methylation sites were then subjected to further differential analysis to determine which *R. fluitans* form a given site dominated. Differential methylation sites (DMSs) were identified based on the proportion of methylated reads to unmethylated reads using the Wilcoxon test and Benjamini–Hochberg p-value correction (padj), as well as stoichiometry (the ratio of methylated reads to other reads at a given position). The significance thresholds were padj < 0.05 and an absolute value of Stoichiometry difference (Stoichiometry diff) > 0.1. DMSs were designated as higher when the stoichiometry difference was greater than 0.1 (indicating higher stoichiometry in the aquatic form of *R. fluitans*) and as lower when the stoichiometry difference was less than 0.1 (indicating higher stoichiometry in the terrestrial form of *R. fluitans*). Additionally, Pearson's correlation was plotted for the intersected methylation sites, analyzing the stoichiometry of these sites in the terrestrial and aquatic forms. The gene *rps12* was excluded from the plastome analyses because its intron extends over a substantial portion of the plastid genome. Because native total DNA was sequenced, organellar reads were identified bioinformatically by mapping to the *R. fluitans* plastome and mitogenome references. Different plastid types within a plant (e.g., chloroplasts vs. non-photosynthetic plastids) share the same plastome sequence; therefore, the plastome methylation profiles reported here reflect the aggregate plastid genome pool present in the sampled thalli, which are predominantly chloroplast-containing tissues.

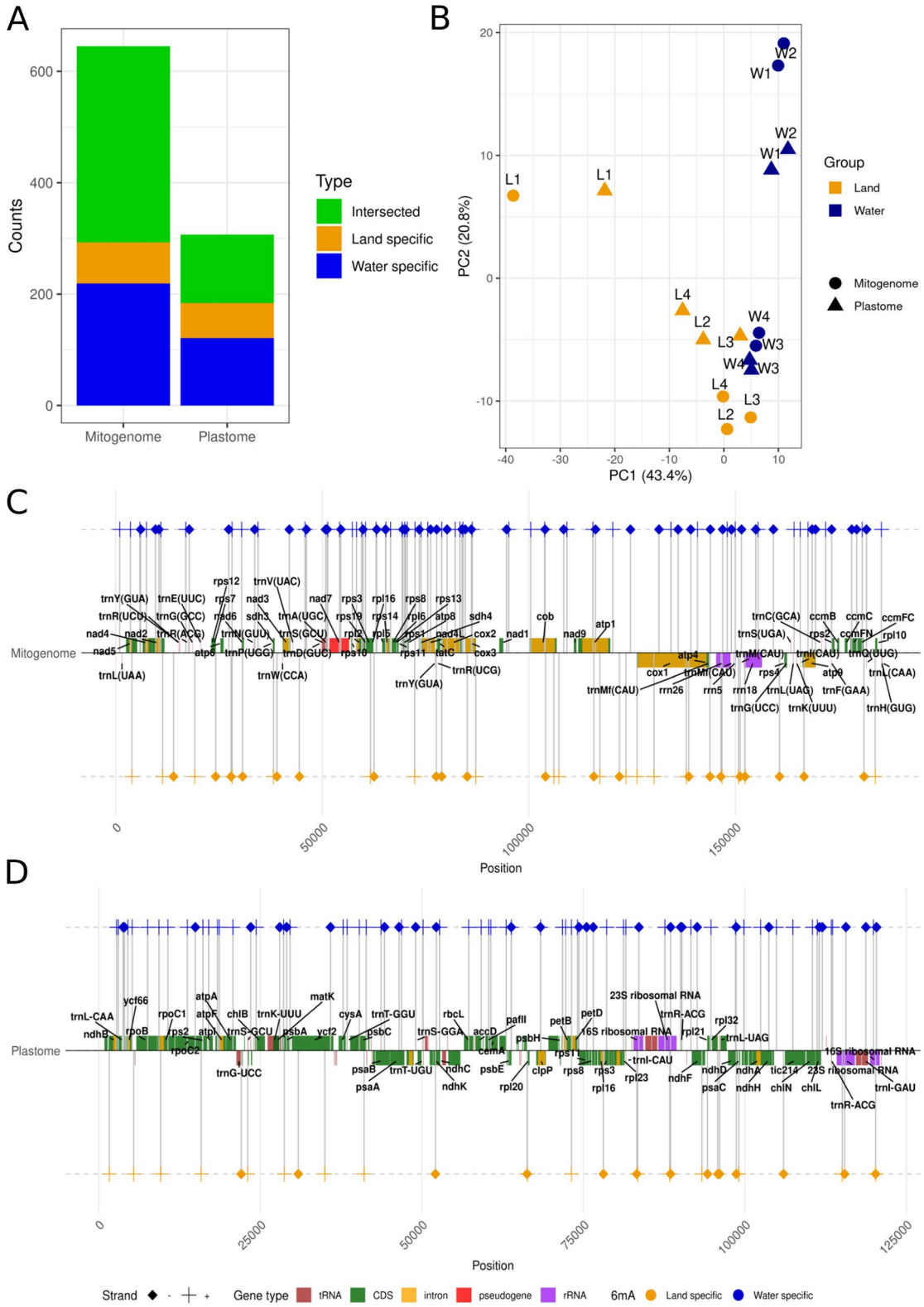

Differential expression analysis

RNA-seq reads were trimmed using the Trimmomatic

◂**Fig. 1** Distinct methylation profiles in the mitogenome and plastome of terrestrial and aquatic *R. fluitans*. **A.** Barplots showing the number of methylation events in the plastome and mitogenome of *R. fluitans*. Shared methylation events across both environments are shown in green, while those specific to the terrestrial environment are shown in yellow and those specific to the aquatic environment are shown in blue. **B.** A graphical representation of the principal component analysis (PCA). The PC1 value is shown on the x-axis, and the PC2 value is shown on the y-axis. Mitochondrial methylation samples are represented by circles, while plastid methylation samples are represented by triangles. Additionally, aquatic samples are colored blue and terrestrial samples are colored orange. **C-D.** Distribution plots of 6 mA methylation events in the mitogenome **(C)** and plastome **(D).** Blue points refer to methylation events specific to the aquatic environment, and orange points refer to those specific to the terrestrial environment. The shape of the points corresponds to their location: crosses represent methylation on the forward (+) strand, while diamonds represent methylation on the reverse (-) strand. Gene annotations are categorized by color: CDS (green), intron (orange), pseudogene (red), tRNA (brown), and rRNA (purple)

v.0.39 tool (Bolger et al. 2014). Subsequently, the Bowtie2 v.2.4.5 tool (Langmead & Salzberg 2012) was used to map the sequences to the mitochondrial and plastid genomes of *R. fluitans*. Information regarding differential gene expression was then obtained using the R libraries txdbmaker v.1.0.1 (https://github.com/Bioconductor/txdbmaker), Rsubread v.2.18.0 (Liao et al. 2019), and edgeR v.4.2.2 (Robinson et al. 2009). Genes with a padj < 0.05 and an absolute log2FoldChange (log2FC) > 0.54 were considered differentially expressed genes (DEGs). From this analysis, tRNA genes in both genomes and rRNA in the plastome were excluded. DEGs with a log2FC less than 0.54 were described as downregulated (higher expression in terrestrial *R. fluitans*), while genes with a log2FC greater than 0.54 were described as upregulated (higher expression in the aquatic form of *R. fluitans*).

Visualization

Visualizations were performed using the R libraries ggplot2 v.3.5.2 (Valero-Mora 2010) and ComplexHeatmap v.2.20.0 (Gu et al. 2016).

Results

Differential DNA methylation patterns in the mitogenome and plastome of terrestrial and aquatic *Riccia fluitans*

The analysis of read mapping results to organellar genomes revealed considerable variance in sequencing depth among the eight *R. fluitans* samples, with plastome reads consistently outnumbering mitochondrial reads. Plastome-mapped reads ranged from 121 188 in Sample L1 (622.88 × coverage) to 16 502 769 in Sample W3 (7 914.79 × coverage), whereas mitochondrial reads were lowest in Sample L1 (42 044 reads, 122.996 ×) and highest in Sample W3 (2 719 788 reads, 4 777.82 ×). Samples L2 and L3 showed similarly high plastome depths of 6 100 464 (7 382.22 ×) and 11 820 298 (7 438.09 ×), respectively, with corresponding mitochondrial coverages of 1 385.19 × (672 374 reads) and 1 354.74 × (1 189 466 reads). Sample L4 mapped 1 964 711 plastome reads at 5 957.23 × and 273 945 mitochondrial reads at 780.677 ×. Among the water-derived samples, W1 achieved 2 995 380 plastome reads (7 387.19 ×) and 272 438 mitochondrial reads (1 019.81 ×), while W2 yielded 3 564 524 plastome reads (7 894.53 ×) and 376 578 mitochondrial reads (2 305.14 ×). The most extensive data were produced by Samples W3, L3, and W4, each exceeding nine million plastome-mapped reads: W3 with 16 502 769 reads (7 914.79 ×) and 2 719 788 mitochondrial reads (4 777.82 ×), L3 with 11 820 298 reads (7 438.09 ×) and 1 189 466 reads (1 354.74 ×), and W4 with 9 290 389 reads (7 911.63 ×) and 1 484 200 reads (3 053.77 ×) (Table 1).

In the course of DNA methylation analysis, a total of 645 6 mA modifications were identified in the mitochondrial genome of *R. fluitans*, while 301 were detected in the plastid genome. Further analysis revealed that 74 modifications in the mitogenome and 63 in the plastome were specific to the terrestrial form, and 219 in the mitogenome and 121 in the plastome were specific to the aquatic form. Additionally, 352 common positions were identified in the mitogenome and 123 in the plastome, which showed methylation in both forms. The ratio of water-specific 6 mA to intersected sites was higher in the plastid than in the mitochondrion (0.98 vs 0.62 in *R. fluitans*), suggesting a greater plastome response to flooding stress (Fig. 1A, Supplemental Table 1).

Principal component analysis (PCA) revealed a clear separation of samples between the aquatic and terrestrial *R. fluitans* in both the mitochondrial and plastid genomes. A high degree of similarity was observed among samples W1, W2, W3, and W4 in both the plastome and mitogenome (Fig. 1B).

Specific to the mitogenome, 36 methylation events were detected on the reverse strand and 38 on the forward strand of terrestrial *R. fluitans*. In the aquatic form of *R. fluitans*, 111 and 108 methylation events were detected on the reverse and forward strands, respectively. In contrast, plastome-specific methylation events were identified as 26 on the reverse and 37 on the forward strand in terrestrial *R. fluitans*, while 42 and 79 events were found on the reverse and forward strands, respectively, in the aquatic form. (Fig. 1C, 1D, Supplemental Table 1).

Common methylation events for both environments were analyzed for statistical significance and stoichiometry variation to identify only the most relevant positions. A total of 14 mitochondrial DMSs on the negative (−) strand and 11

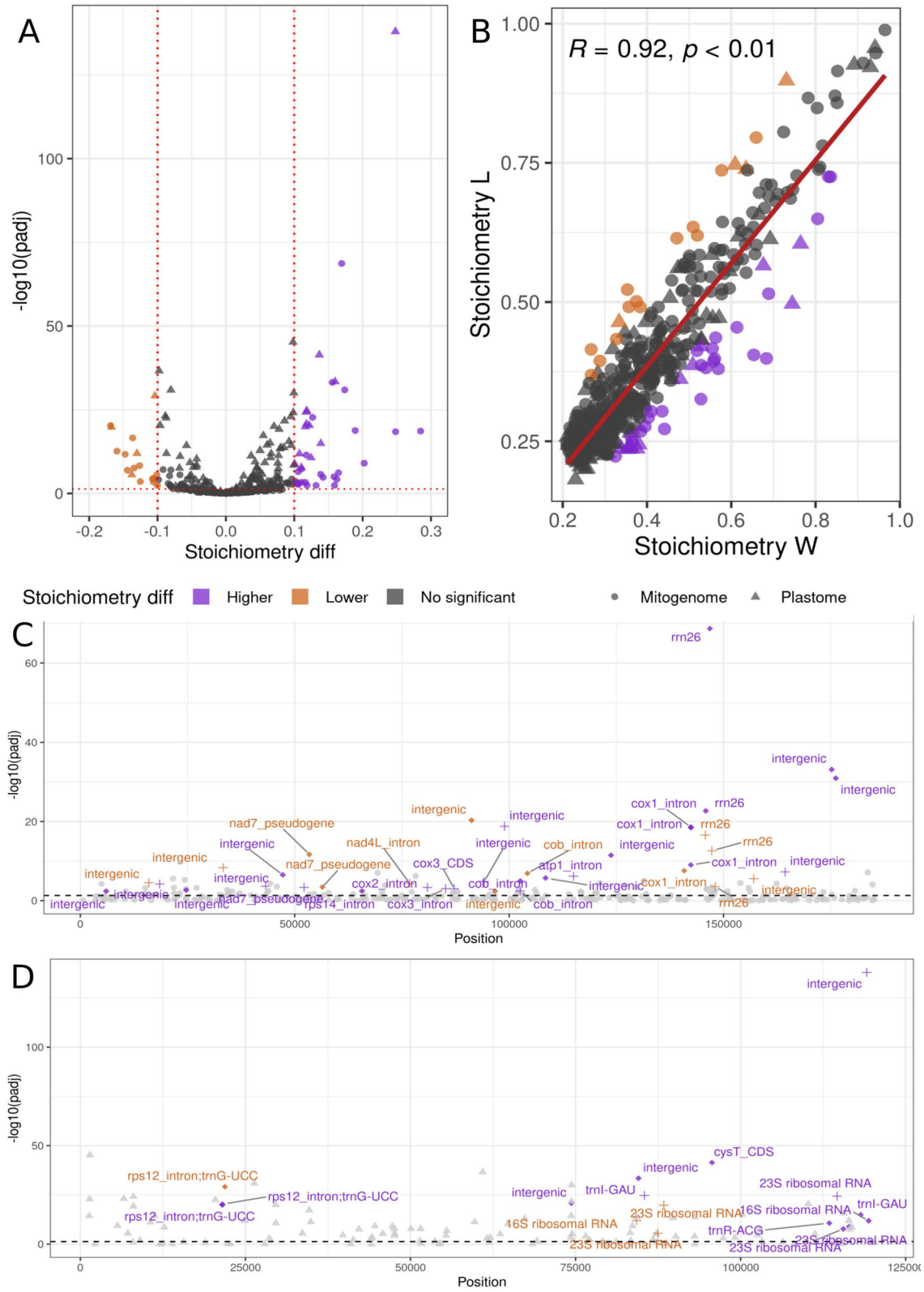

on the positive (+) strand were identified with higher stoichiometry. Conversely, seven mitochondrial DMSs on the positive (+) strand and six on the negative (−) strand were

◂**Fig. 2** Analysis of shared 6 mA methylation positions. **A** A volcano plot showing the distribution of methylation data. The x-axis represents the stoichiometric difference, while the y-axis represents the -log10(padj). **B** A scatter plot comparing the stoichiometry of terrestrial (L) samples on the y-axis with the stoichiometry of aquatic (W) samples on the x-axis. Circles represent methylation detected in the mitochondrion, while triangles represent methylation detected in the plastome. The colors of the points indicate their stoichiometry: brown for lower stoichiometry, purple for higher stoichiometry, and gray for statistically insignificant positions. **C-D.** A Manhattan plot illustrating methylation in the mitogenome **(C)** and plastome **(D)**. The colors of the points correspond to their stoichiometric character: brown for lower, purple for higher, and gray for no significant difference. Statistically significant points are shaped as a plus sign (+) if located on the forward strand and as a diamond if located on the reverse strand

identified with lower stoichiometry. In the plastome, ten higher stoichiometry DMSs were assigned to the negative (−) strand and three to the positive (+) strand, while three lower stoichiometry DMSs were identified on the positive (+) strand and one on the negative (−) strand (Fig. 2A, B, C, and D, Supplemental Table 1).

Gene expression differences in organellar genomes of terrestrial and aquatic R. fluitans

PCA revealed a clear separation of aquatic and terrestrial samples based on gene expression in both the mitochondrial and plastid genomes (Fig. 3A). Through differential expression analysis, six DEGs were identified: one in the mitogenome and five in the *R. fluitans* plastome. The mitochondrial DEG, *rrn5*, was found to have the lowest expression among the organelle genomes and showed higher expression in the aquatic form of *R. fluitans*. Among the plastome DEGs, *cysA*, *rps15*, *rpl32*, and *accD* were all upregulated, exhibiting higher expression in the aquatic form. In contrast, *psbA*, another DEG, was the most highly expressed gene in the organelle genomes and was the only DEG that was downregulated, showing higher expression in the terrestrial form of *R. fluitans* (Fig. 3B, C, D, and E, Supplemental Table 2).

Discussion

In this study, the expression profiles and 6 mA methylation were compared between the aquatic and terrestrial forms of *R. fluitans* in their organellar genomes. The results showed robust 6 mA characteristics in the organellar genomes of *R. fluitans* and differentiated expression between the aquatic and terrestrial forms of the plant.

The aquatic morphotype of *R. fluitans* exhibited a consistently higher density of 6 mA sites in both organellar genomes compared with the terrestrial morphotype (Fig. 1A, 1C, 1D, 2A, 2B, 2C, 2D, Supplemental Table 1), suggesting that environmental conditions modulate adenine methylation at a genome-wide level. This pattern parallels previous findings at the RNA modification level, supporting a coordinated epigenetic and epitranscriptomic response to habitat transition. In previous studies conducted at the RNA level, the aquatic form of *R. fluitans* was found to exhibit more Ψ, m6A, and m5C positions, as well as global elongation of poly(A) tails in nuclear genome transcripts compared to the terrestrial form (Maździarz et al. 2024; Maździarz et al. 2025a, b). This indicated that epitranscriptomic processes were more abundant in the aquatic environment for this plant, suggesting a potentially active stress memory mechanism that was triggered in the aquatic environment. This pattern was similarly observed at the epigenetic level in both plastomes and mitogenomes, where 6 mA methylations were increased. Therefore, examination of DNA methylation in the nuclear genome of *R. fluitans* could prove to be an interesting topic for future research on this amphibious plant.

The plastome typically exhibits significantly higher coverage and a greater number of mapped reads than the mitogenome (Morley & Nielsen 2016; Shen et al. 2019). A higher number of 6 mA methylation events was observed in the mitogenome than in the plastome, accompanied by lower plastome coverage (Fig. 1A, Table 1, Supplemental Table 1). This contrasts with findings in *A. thaliana*, where the 6 mA density was reported to be higher in the plastid than in the mitochondrion (Li et al. 2020b; Yuan et al. 2020b). This may have been caused by the differences in lengths between the plastome and mitogenome of *R. fluitans* and *A. thaliana* (Unseld et al. 1997; Sato et al. 1999; Kwon et al. 2019; Min et al. 2020).

Among the differentially expressed genes (DEGs), *accD* was characterized by an increased expression in the aquatic form of *R. fluitans* (Fig. 3C, Supplemental Table 2) and was also found to have two water-specific 6 mA methylations within the CDS region (Fig. 3D, Supplemental Table 1). In tobacco, *accD* was shown to be essential for leaf development and cell viability, and knockout mutants of the gene were found to exhibit pale-green sectors and an abnormal leaf lamina due to inhibited cell division (Kode et al. 2005). Gene *accD* knockout studies in the plastome were shown to result in impaired plastome division, reduced seed set, and altered storage metabolism. Paradoxically, this also promoted heterotrophic growth despite a decrease in photoautotrophic growth (Caroca et al. 2021).

In the terrestrial form of *R. fluitans*, *psbA* showed significantly higher expression and was the most highly expressed among all plastid genes (Fig. 3C, Supplemental Table 2). Additionally, four water-specific 6 mA methylations were identified within this gene (three on the (+) strand and one on the (-) strand), along with one land-specific 6 mA methylation on the forward strand (Fig. 1D, Supplemental Table 1). The *psbA* gene, which is known to be involved in

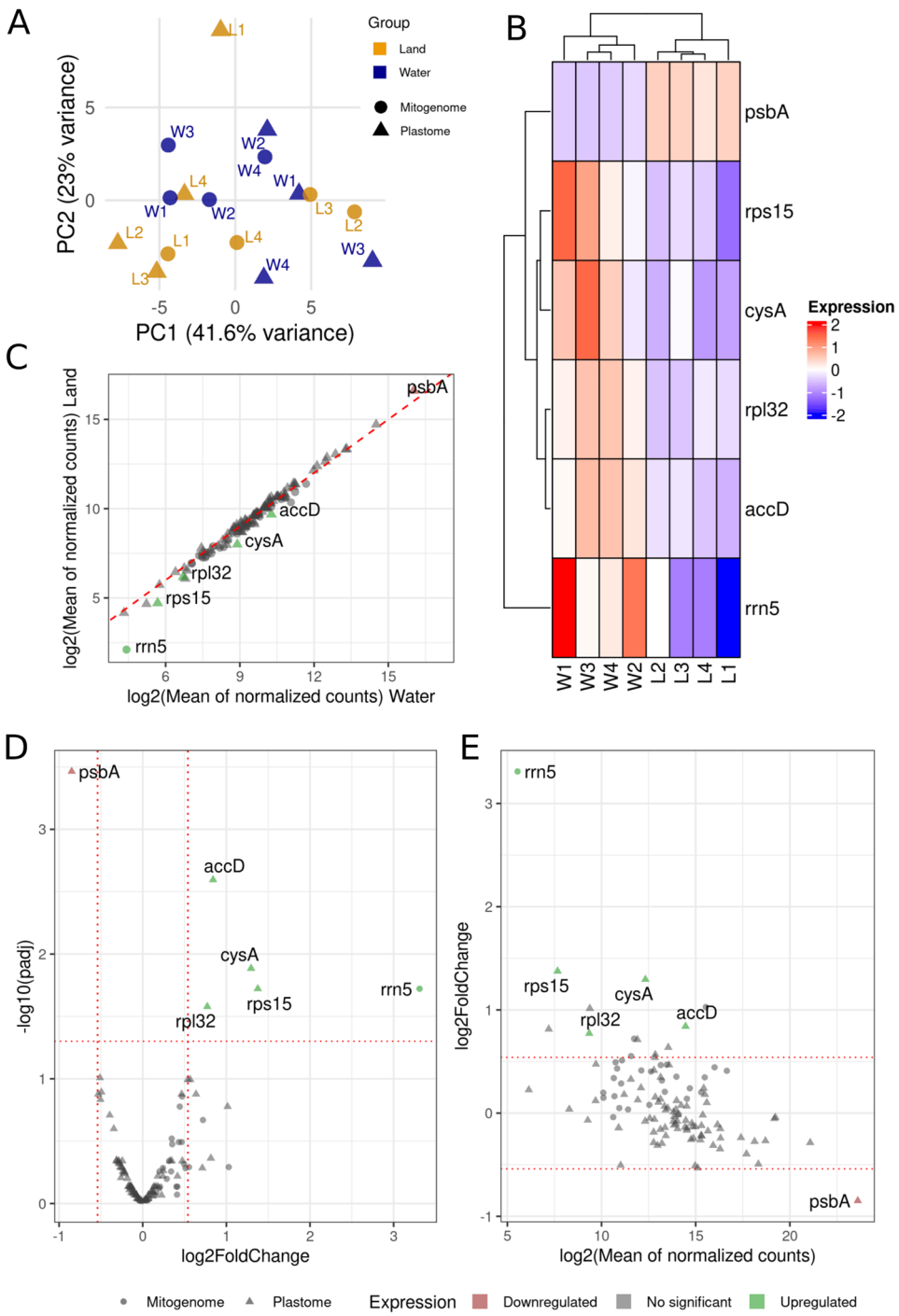

Fig. 3 PCA and differential gene expression analysis of *R. fluitans* organellar genomes. Points represented by circles indicate mitochondrial genes, while points represented by triangles indicate plastid genes. **A.** Graphical representation of the PCA. The PC1 value is shown on the x-axis, and the PC2 value is shown on the y-axis. Blue points represent the aquatic form of *R. fluitans*, while orange points represent the terrestrial form. **B.** Heatmap of the six DEGs, representing the z-score of normalized counts according to the scale, where darker blue indicates negative values and darker red indicates positive values. **C.** Scatter plot of gene expression distribution. The mean expression value in the aquatic form of *R. fluitans* is presented on the x-axis, and the mean expression value in the terrestrial form is shown on the y-axis. The dashed red line represents the line of equality. Red points represent downregulation (higher expression in the terrestrial form), and green points represent upregulation (higher expression in the aquatic form). Gray points are not statistically significant. **D.** Volcano plot illustrating differential gene expression, where the log2FC is plotted on the x-axis and the -log10(padj) is plotted on the y-axis. The dashed red lines indicate the significance thresholds. **E.** MA plot showing the relationship between gene expression level and fold change, where the log2 of the mean of normalized counts is presented on the x-axis and the log2FC is shown on the y-axis

photosynthesis and energy production, has been similarly described in other species such as *Agathis dammara*, *Keteleeria davidiana*, *Cunninghamia konishii*, *Cephalotaxus wilsoniana*, *Sciadopitys verticillata*, and *Nageia nagi* (Wu et al. 2021). The *psbA* gene encodes the D1 subunit of photosystem II, and its high expression level in the plastid is considered a key mechanism for plant adaptation to environmental stress, particularly under conditions of high light intensity. The transcription and translation of the *psbA* gene play a crucial role in high-light stress responses (Zhang et al. 2020). Plastids have been shown to regulate the transcriptional efficiency of *psbA* during photoinhibition in adverse environmental conditions, such as high light and temperature (Pfannschmidt et al. 1999; Danilova et al. 2018). The overexpression of *psbA* in high-altitude-adapted *A. thaliana* Tibet-0 was classified as a photoprotective mechanism in a high light environment (Zhang et al. 2021).

Conclusions

This study provides the first genome-wide evidence of 6 mA methylation in the organellar genomes of *R. fluitans* and demonstrates that methylation patterns differ between aquatic and terrestrial forms. The data indicate that 6 mA may contribute to environmental adaptation through modulation of organellar gene expression. These results introduce an unexplored dimension of plant epigenetic regulation and establish *R. fluitans* as a model for studying the evolution of multi-compartmental methylation systems in early land plants.

A key finding was that a greater amount of 6 mA methylation was observed in the plastome and mitogenome of the aquatic *R. fluitans* form. Additionally, changes in the expression of *psbA* (higher expression in the terrestrial form) and *accD* (higher expression in the aquatic form) were also observed. While epigenetic and transcriptomic changes in the organellar genomes were highlighted by these results, further research including the nuclear methylome was considered essential to fully understand the coordination and epigenetic cross talk between these compartments.

Supplementary Information The online version contains supplementary material available at https://doi.org/10.1007/s00299-026-03775-z.

Acknowledgements The study was financially supported by The National Science Center Kraków, Poland: Grant No. 2020/39/B/NZ8/02504.

Author contribution The conceptualization of the study was carried out by MM and JS. The investigation was conducted by KK and PS. The software used in the study was developed by MM. Formal analysis was performed by MM. The methodology was designed by MM, KK, PS, and JS. The original draft of the writing was prepared by all authors. Review and editing of the writing were done by MM, KK, and JS. JS provided supervision for the project, managed its administration, and secured the necessary funding.

Funding Narodowe Centrum Nauki, 2020/39/B/NZ8/02504, Jakub Sawicki

Data availability The BAM and FASTQ files have been deposited into the ENA EMBL-EB database under accession numbers PRJEB100580 and PRJEB72692.

Declarations

Conflict of interest The authors state there is no conflict of interest.

References

Althoff F, Zachgo S (2020) Transformation of Riccia fluitans, an Amphibious Liverwort Dynamically Responding to Environmental Changes. Int J Molecul Sci 21(15):5410

Althoff F, Wegner L, Ehlers K, Buschmann H, Zachgo S (2022) Developmental Plasticity of the Amphibious Liverwort Riccia fluitans. Front Plant Sci 13:909327

Arora H, Singh RK, Sharma S, Sharma N, Panchal A, Das T, Prasad A, Prasad M (2022) DNA methylation dynamics in response to abiotic and pathogen stress in plants. Plant Cell Rep 41:1931–1944. https://doi.org/10.1007/s00299-022-02901-x

Bolger AM, Lohse M, Usadel B (2014) Trimmomatic: a flexible trimmer for Illumina sequence data. Bioinformatics 30(15):2114

Caroca R, Howell KA, Malinova I, Burgos A, Tiller N, Pellizzer T, Annunziata MG, Hasse C, Ruf S, Karcher D, Bock R (2021) Knockdown of the plastid-encoded acetyl-CoA carboxylase gene uncovers functions in metabolism and development. Plant Physiol 185:1091–1110. https://doi.org/10.1093/plphys/kiaa106

Clark JW, Harris BJ, Hetherington AJ, Hurtado-Castano N, Brench RA, Casson S, Williams TA, Gray JE, Hetherington AM (2022) The origin and evolution of stomata. Current Biol 32(11):539–553

Danilova MN, Kudryakova NV, Andreeva AA, Doroshenko AS, Pojidaeva ES, Kusnetsov VV (2018) Differential impact of heat stress on the expression of chloroplast-encoded genes. Plant Physiol Biochem 129:90–100

Gu Z, Eils R, Schlesner M (2016) Complex heatmaps reveal patterns and correlations in multidimensional genomic data. Bioinformatics 32:2847–2849. https://doi.org/10.1093/bioinformatics/btw313

Karst SM, Ziels RM, Kirkegaard RH, Sørensen EA, McDonald D, Zhu Q, Knight R, Albertsen M (2021) High-accuracy long-read amplicon sequences using unique molecular identifiers with Nanopore or PacBio sequencing. Nat Methods 18:165–169

Kode V, Mudd EA, Iamtham S, Day A (2005) The tobacco plastid accD gene is essential and is required for leaf development. Plant J 44:237–244. https://doi.org/10.1111/j.1365-313X.2005.02533.x

Kwon W, Min J, Xi H, Park J (2019) The complete chloroplast genome of *Riccia fluitans* L. (Ricciaceae, Marchantiophyta). Mitochondrial DNA B 4:1895–1896 ((**accessed 20 October 2025**))

Langmead B, Salzberg SL (2012) Fast gapped-read alignment with Bowtie 2. Nat Methods 9:357 ((**accessed 20 October 2025**))

Li H, Handsaker B, Wysoker A, Fennell T, Ruan J, Homer N, Marth G, Abecasis G, Durbin R (2009) The sequence alignment/map format and SAMtools. Bioinformatics 25:2078–2079. https://doi.org/10.1093/bioinformatics/btp352. ((**accessed 20 October 2025**))

Li Y, Zhang XM, Luan MW, Xing JF, Chen J, Xie SQ (2020) Distribution patterns of DNA N6-methyladenosine modification in non-coding RNA genes. Front Genet 11:516058 ((**accessed 20 October 2025**))

Liao Y, Smyth GK, Shi W (2019) The R package Rsubread is easier, faster, cheaper and better for alignment and quantification of RNA sequencing reads. Nucleic Acids Res 47:e47–e47. https://doi.org/10.1093/nar/gkz114. ((**accessed 20 October 2025**))

Liu J, He Z (2020) Small DNA methylation, big player in plant abiotic stress responses and memory. Front Plant Sci 11:595603 ((**accessed 20 October 2025**))

Liu N, Ding Y, Fromm M, Avramova Z (2014) Different gene-specific mechanisms determine the 'revised-response' memory transcription patterns of a subset of *A. thaliana* dehydration stress responding genes. Nucleic Acids Res 42:5556–5566. https://doi.org/10.1093/nar/gku220. ((**accessed 20 October 2025**))

Maździarz M, Krawczyk K, Kurzyński M, Paukszto Ł, Szablińska-Piernik J, Szczecińska M, Sulima P, Sawicki J (2024) Epitranscriptome insights into *Riccia fluitans* L. (Marchantiophyta) aquatic transition using nanopore direct RNA sequencing. BMC Plant Biol 24:1–16 ((**accessed 20 October 2025**))

Maździarz M, Krawczyk K, Szablińska-Piernik J, Paukszto Ł, Szczecińska M, Sulima P, Sawicki J (2025a) Epitranscriptomic and expression profiling in *Riccia fluitans* across diverse environmental conditions. Comput Struct Biotechnol J 27:4232 ((**accessed 20 October 2025**))

Maździarz M, Paukszto Ł, Sawicki J (2025b) TAILcaller: an R package for analyzing differences in poly(A) tail length for Oxford Nanopore RNA sequencing. Bioinformatics Adv 5:vbaf235. https://doi.org/10.1093/bioadv/vbaf235. ((**accessed 20 October 2025**))

Min J, Kwon W, Xi H, Park J (2020) The complete mitochondrial genome of *Riccia fluitans* L. (Ricciaceae, Marchantiophyta): investigation of intraspecific variations on mitochondrial genomes of R. fluitans. Mitochondrial DNA B 5(2):1220–1222

Morley SA, Nielsen BL (2016) Chloroplast DNA copy number changes during plant development in organelle DNA polymerase mutants. Front Plant Sci 7:171196 ((**accessed 20 October 2025**))

Paukszto Ł, Górski P, Krawczyk K, Maździarz M, Szczecińska M, Ślipiko M, Sawicki J (2023) The organellar genomes of Pellidae (Marchantiophyta): the evidence of cryptic speciation, conflicting phylogenies and extraordinary reduction of mitogenomes in simple thalloid liverwort lineage. Sci Rep 13:1–17 ((**accessed 20 October 2025**))

Pfannschmidt T, Nilsson A, Tullberg A, Link G, Allen JF (1999) Direct transcriptional control of the chloroplast genes psbA and psaAB adjusts photosynthesis to light energy distribution in plants. IUBMB Life 48:271–276 ((**accessed 20 October 2025**))

Rang FJ, Kloosterman WP, de Ridder J (2018) From squiggle to basepair: computational approaches for improving nanopore sequencing read accuracy. Genome Biol 19:1–11 ((**accessed 20 October 2025**))

Robinson MD, McCarthy DJ, Smyth GK (2009) edgeR: a Bioconductor package for differential expression analysis of digital gene expression data. Bioinformatics 26:139 ((**accessed 20 October 2025**))

Sato S, Nakamura Y, Kaneko T, Asamizu E, Tabata S (1999) Complete structure of the chloroplast genome of *Arabidopsis thaliana*. DNA Res 6(5):283–290. https://doi.org/10.1093/dnares/6.5.283

Sawicki J, Krawczyk K, Kurzyński M, Maździarz M, Paukszto Ł, Sulima P, Szczecińska M (2023) Nanopore sequencing of organellar genomes revealed heteroplasmy in simple thalloid and leafy liverworts. Acta Soc Bot Pol 92:1–13 ((**accessed 20 October 2025**))

Shen J, Zhang Y, Havey MJ, Shou W (2019) Copy numbers of mitochondrial genes change during melon leaf development and are lower than the numbers of mitochondria. Hortic Res 6:s41438-019-0177-8. https://doi.org/10.1038/s41438-019-0177-8. ((**accessed 20 October 2025**))

Unseld M, Marienfeld JR, Brandt P, Brennicke A (1997) The mitochondrial genome of *Arabidopsis thaliana* contains 57 genes in 366,924 nucleotides. Nat Genet 15(1):57–61

Valero-Mora PM (2010) ggplot2: elegant graphics for data analysis. J Stat Softw 35:1–3 (**[online] URL: (accessed 20 October 2025**))

Wang Y, Zhao Y, Bollas A, Wang Y, Au KF (2021) Nanopore sequencing technology, bioinformatics and applications. Nat Biotechnol 39(11):1348–1365

Wu CS, Sudianto E, Chaw SM (2021) Tight association of genome rearrangements with gene expression in conifer plastomes. BMC Plant Biol 21:1–8. https://doi.org/10.1186/s12870-020-02809-2

Yuan DH, Xing JF, Luan MW, Ji KK, Guo J, Xie SQ, Zhang YM (2020) DNA N6-Methyladenine modification in wild and cultivated soybeans reveals different patterns in nucleus and cytoplasm. Front Genet 11:516612 (**[online] URL: (accessed 20 October 2025**))

Zhang M, Zhao J, Li W, Wen S, Huang H, Dong J, Liu B, Zhang G, Wang HB, Shen Y, Jin HL (2021) Increased photosystem II translation efficiency as an important photoprotective mechanism in an *Arabidopsis thaliana* ecotype (Tibet-0) adapted to high light environments. Environ Exp Bot 183:104350 (**[online] URL: (accessed 20 October 2025**))

Zhang Y, Zhang A, Li X, Lu C (2020) The Role of Chloroplast Gene Expression in Plant Responses to Environmental Stress. Int J Molecul Sci 21:6082

Authors and Affiliations

Mateusz Maździarz[1] · Katarzyna Krawczyk[1] · Paweł Sulima[2] · Jakub Sawicki[2]

✉ Mateusz Maździarz
mateusz.mazdziarz@uwm.edu.pl

[1] Department of Botany and Evolutionary Ecology, University of Warmia and Mazury in Olsztyn, Plac Łódzki 1, 10-719 Olsztyn, Poland

[2] Department of Genetics and Plant Pathophysiology, University of Warmia and Mazury in Olsztyn, Plac Łódzki 3, 10-724 Olsztyn, Poland